J. Inst. Eng. India Ser. D (January–June 2022) 103(1):161–171
https://doi.org/10.1007/s40033-021-00326-6

ORIGINAL CONTRIBUTION

Experimental Investigations on Microstructure and Mechanical Properties of Retrogression and Reaging (RRA)-Treated AA7075 (Al-Zn-Mg) Alloy

T. Pavan Tejasvi[1] · H. M. Somashekar[1] · V. Ranjith[1]

Received: 24 October 2021 / Accepted: 16 December 2021 / Published online: 23 February 2022

Abstract This paper reports on mechanical microstructure and mechanical properties of AA7075 alloy subjected to retrogression and reaging process (RRA). The AA7075 alloy was homogenized for two hours at 460 °C and aged for 24 h in a furnace set to 120 °C followed by retrogression process. The aged specimens were retrograted for 3 min, 7 min, 9 min, and 11 min at temperatures of 140, 160, 180, 200 and 220 °C. These retrogressed specimens are subjected to reaging for 24 h at a temperature of 120 °C. Microstructural changes are investigated using X-ray diffraction (XRD) as well scanning electron microscopy (SEM). According to XRD analysis, precipitates are formed in the microstructure of RRA-treated AA7075, consisting of $MgZn_2$ precipitates. The hardness and tensile strength increase at first, then drop as the temperature rises. A decline in hardness and tensile strength can be seen as the retrogression period increases. Elongation was highest at 160 °C over the entire retrogression period. However, the percentage elongation decreases as the temperature rises, regardless of the length of time.

Keywords Retrogression · Reaging · AA7075 alloy · Mechanical properties

Introduction

Because of the unique properties of material, the aluminum can be used in a wide range of applications. Aluminum has good formability, a conductivity that is significantly superior to both thermal and electrical conductivity, and a high strength-to-weight ratio, all these make the aluminum to be attractive in the industry. In a variety of engineering applications, especially in the place of metals and wood, the alloy usage has seen widespread over the last few years. Because of its high weight-to-strength ratio, in aircraft applications the aluminum–zinc–magnesium alloy can be age hardened as well as heat treated. As far as heat-treatable alloys are concerned, this standard structural alloy is said to be the utmost versatile, as well as most suitable for moderate to greater strength necessities as well as holds a better toughness characteristic. To the conditions of atmosphere as well as to the sea water, the 7075 alloy offers a strong corrosion resistance [1–8]. Wherever the cosmetic appearance is crucial, this alloy responds well to anodizing as well as provides better finishing characteristics. After all the 7075 is a heat-treatable alloy, so the welding as well as joining of the alloy 7075 is done easily using a variety of commercial techniques. Because of its excellent strength-to-density ratio, the alloys of 7000 series like AA7075 are frequently utilized in transportation applications such as aviation, automotive as well as marine. In other areas also, their lightweight as well as strength is essential. AA7075 is extensively used in making the hang glider airframes, components of bicycle, as well as rock climbing equipment. For the US military, the M16 rifles manufacture is one noteworthy application for AA7075. For fork sets, camping knife as well as for lacrosse sticks in shafts, it is most frequently used. For the precision rifles the French

✉ T. Pavan Tejasvi
pvn.tejasvi@gmail.com

[1] Dr. Ambedkar Institute of Technology, Bangalore, India

armament industry PGM as well as Desert Tactical Arms uses it. AA7075 is commonly utilized in the production of mold tool because of its thermal characteristics as well as its ability to be finely polished, also due to its strength as high density. Heat treatment for reaging as well as retrogression is carried out in three steps: retrogression, reaging, solutionization, and age hardening. A type of heat treatment which is utilized to strengthen metal alloys in metallurgy is aging as well as solutionization. By forming precipitates or solid impurities it strengthens the metal, which is why it is also known as precipitation hardening. The name of its derives from aging point of the metal during the hardening process, precipitates can be generated whether by storing it for an prolonged period of time at low temperature or heating it for a prolonged period of time prior to usage. Aluminum alloys in the 2000 series, 6000 series, as well as 7000 series are precipitation hardening alloys examples [9–16].

Although new aluminum alloys and the updated version of old alloys are continuously developed, the corrosion-induced deterioration, and also further exfoliation as well as SCC affects numerous aircraft structures as well as components made of 7xxx-T6. Considering the age of most military fleets as well as many commercials, the issue seems to have become crucially influential. All over the world, these aging's maintenance cost is a serious issue. Reaging as well as retrogression (RRA) is a two-step heat treatment, high resistance to corrosion has been shown to be equivalent to T73 in aluminum alloys 7xxx, combined with the levels of T6 strength. As a result, the method has a lot of promise as a way to prevent damages by corrosion in the components of aircraft which is produced by the T6 material.

At varied temperatures and times, Gokhen et al. [7] conducted the retrogression technique to AA7075 alloy. Age treatment was restarted with T6 settings after the retrogression. Electrical conductivity tests were used to detect the mechanical qualities of aged samples, as well as the physical attributes of samples. Precipitates at the grain boundary are linked to the effects of temperature and reagent time on impact toughness and hardness.

Esmailian et al. [8] evaluated the RRA heat treatment and the influence of RRA duration for AA7075 alloy on mechanical properties. The results reveal that the AA7075 alloy's retrogression and final strength rise significantly over a 40-min period.

During retrogression and retrogression plus aging, Dahn et al. [15] have reported on microstructural changes in AA7075 alloy, and how these changes affect mechanical characteristics. As a result of G.P. zones partially dissolving, strength decreased in the early stages of retrogression, but quickly recovered once the growth of semi-coherent was established. Retrogression and reaging, it is hypothesized, increased the volume fraction of G.P. zones and particularly precipitates in both the T6 and retrogressed circumstances, hence greatly enhancing the alloy's strength.

The microstructure of AA7075 alloy in the T651 temper was examined by Park et al. [16] to see how RRA treatments affected the matrix and grain boundaries. Small particles of the transition phase dissolve during the retrogression treatment, resulting in the bigger particles of undergoing transformation into, while the three common variants of phase precipitates coarsen and new phase particles precipitate, especially the first variant. Precipitation of the proliferation of partially dissolving particles is the key processes that occur during the reaging procedure. 7075 alloy in RRA temper has a high strength because of the high concentration of particles in this dispersion.

Microstructure variations in alloys are well recognized to have a serious influence on their mechanical characteristics. In order to generate high-performance industrial alloys (such as hardness yield strength as well as toughness), it is essential to comprehend the relationship between the techniques of thermomechanical used performed as well as the mechanical qualities achieved. With impact toughness the relationship between hardness changes as well as tensile strength had been still not completely described despite numerous researches on this issue [16–22]. The samples of T651 have been processed under RRA condition as per the certain conditions in this investigation. Under RRA conditions, at different temperature some of the tests such tensile strength, hardness as well as analysis of microstructure were performed. The study's main goal is to determine the cause of the shift in mechanical properties.

Materials and Methods

The material selected for the study is Al-Zn-Mg (7075) alloy received from Hindustan Aeronautical Limited (HAL), Bangalore, India. Chemical composition of the alloy has been carried by chemical analysis optical emission spectroscopy (OES) test. The chemical analysis of the raw material has been done to confirm that it is the 7075 aluminum alloy specimen. The raw material obtained in the semicircular block is a casted one and exposed to solutionizing process. In this method the alloy was heated in the furnace at the temperature of 460 °C for the time interval of 2 h. The next step is water quenching to relieve the residual stresses. The semicircular block is drilled and cut from the circular block.

Heat Treatment

Homogenization process has been carried out for the procured raw materials, in this process the specimens are heated in the furnace at 460 °C for 2 h. The homogenized method is successfully conceded to relieve residual stress from the specimen to attain even microstructure. First, the materials are subjected to aging process at the temperature of 120 °C for 24 h' time interval in the muffle furnace. Retrogression is a heat treatment method in which the specimens are heated in the furnace for 3 min, 7 min, 9 min, and 11 min at varying temperatures of 140, 160, 180, 200 and 220 °C and then cooled in the atmospheric air [8–16]. These retrogressed specimens are again subjected to reaging where the specimens are kept in the furnace for 24 h' time interval at 120 °C. The reaged specimens are then water cooled in 50 L of water bath and after cooling the temperature of water should not increase more than 3 °C.

The standard samples are machined and prepared by cutting the specimen of disk shape of 50 mm diameter and 8 mm thickness. Each sample is part of disk divided into four parts. The dimensions of the samples are 12.5-mm semicircular disk and 3-mm0thick sliced in an electric discharge machine (EDM). The specimens are subjected to retrogression at the temperatures of 140, 160, 180, 200 and 220 °C and then air-cooled to bring the temperature of specimens back to normal room temperature. These specimens are again subjected to reaging at the temperatures of 120 °C at the time interval of 24 h inside the furnace. The specimens are quenched in water and temperature is reduced to room temperature. The phase identification in heat-treated AA7075 alloys was performed using an X-ray diffraction machine (PANalytical's—X'Pert3 Powder). The Rockwell hardness tester was used to determine hardness. For each sample, five indentations were made, and the average of the five results was used to calculate the hardness of each specimen. The ASTM E8M standard was used to carry out tensile tests on treated aluminum 7075 alloy under various heat treatment conditions.

Results and Discussion

The SEM images were studied and compared to those of RRA-treated specimens. Figure 1a-b shows that precipitates formed as a result of RRA treatment are identified as white dots. The specimens are retrograted at temperatures of 140 and 160 °C. These retrogressed precipitates have a semi-coherent one phase. The reaging process has increased the dissolution of one phase, resulting in an increase in the coherent equilibrium phase.

Figure 2a-b shows that the reaging process has increased the dissolution of one phase as a result of RRA treatment. This is the factor that can be seen in the formation of additional precipitates in the reaged AA7075 alloy microstructure. The disintegration of a supersaturated solid solution is caused by the formation of fine intermetallic equilibrium phase particles that spread across the grains, as illustrated in Fig. 3a-b. These intermetallic particles at the grain boundaries are stiffer and more evenly distributed throughout the grain. Increased RRA treatment temperature, i.e., 200 and 220 °C, results in an increase in intermetallics. The alloy has a structure of first-phase and second-phase intermetallics, which improves the mechanical properties of the AA7075. These areas are visible as dark areas in the SEM images below, Fig. 4a-b [23–26]. SEM images of raw AA7075 material without RRA treatment are shown in Fig. 5a-b. These figures show that the precipitate sizes are very small when compared to the sizes of RRA-treated specimens at 140, 160, 180, 200 and 220 °C. The cast specimen has Al + Eutectic phase (black region) as well as Al matrix (light particles) in the grain boundaries, as seen in the microstructure. Because these precipitates are distributed throughout the matrix in the raw material, the tensile strength of raw AA7075 is lower. According to previous SEM images, the effective parameters for increasing the mechanical properties of AA7075 alloy are T6 tempering and reaging, as a result of which larger size clusters of precipitate are spread and secondary intermediate particles (equilibrium phase) have been formed across the grain and grain boundaries of the aluminum matrix.

The as-cast specimen's microstructure includes the -Al + Eutectic phase (dark) in the -Al matrix (light), as well as the eutectic phase at grain boundaries. The solutionized and peak age-hardened microstructures are made up of finely precipitated second-phase components that are uniformly distributed in an aluminum matrix. The precipitates distribution is homogeneous in the age-hardened state. The main precipitates are the non-coherent phase. The retrogression time has been found to increase non-coherent-phase dissolution as well as coherent one-phase precipitation, as shown in Fig. 6a-b. That could be the reason why the material's hardness increases with RRA treatment rather than pre-aging treatment. However, this resulted in a decrease in hardness as well as grain coarsening, as well as an increase in retrogression time.

After RRA treatment, the material gains strength from the T6 condition and corrosion resistance from the T73 condition. This is because RRA treatment causes the firmness of various phases as well as the formation of microstructures. Changes in the microstructure during RRA improve the alloy characteristics in the case of 7075-T6: The following changes have occurred in these

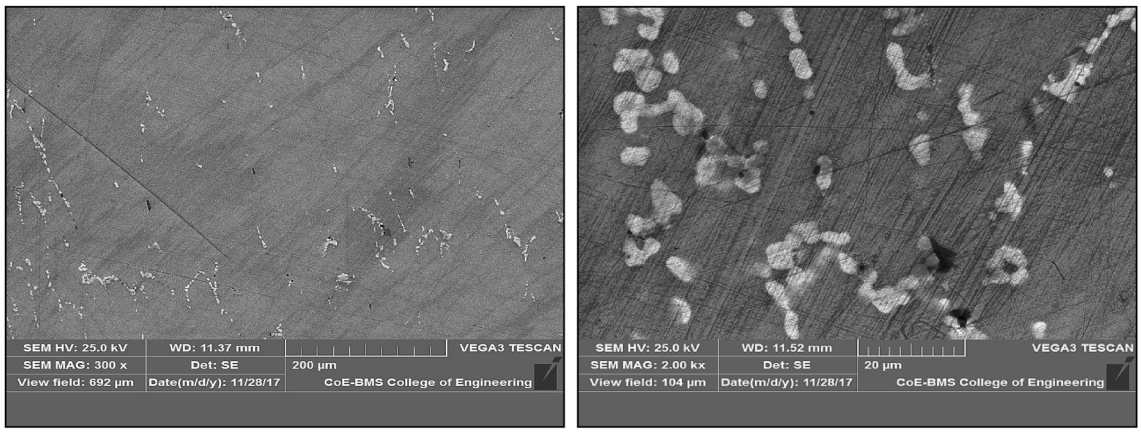

Fig. 1 **a** SEM of RRA-treated Al7075 alloy at 140 ^{o} C

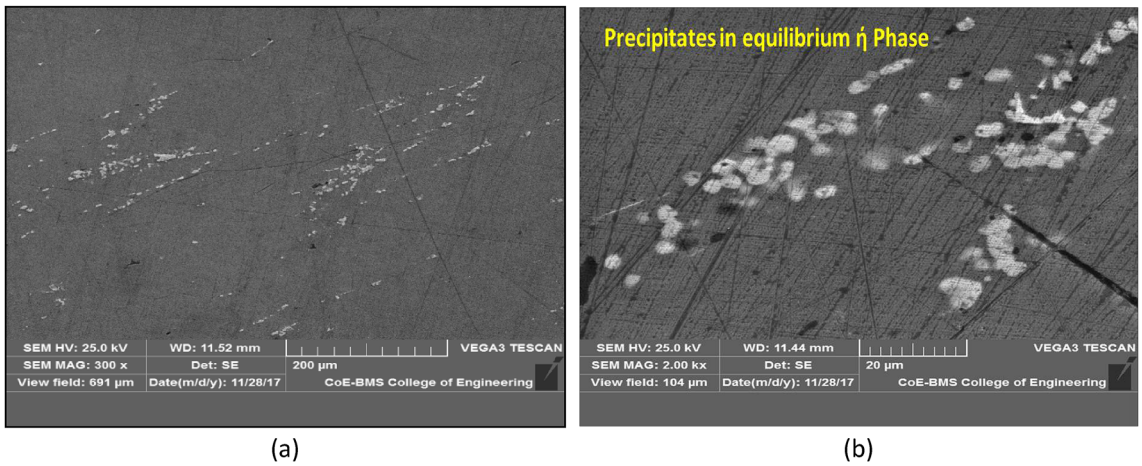

Fig. 2 **a-b** SEM of RRA-treated Al7075 alloy at 160 °C

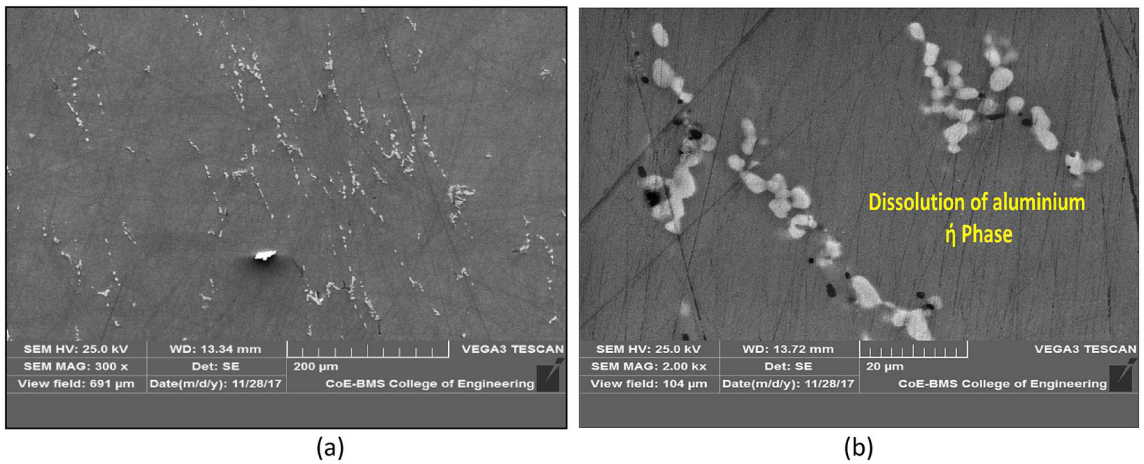

Fig. 3 **a-b** SEM of RRA-treated Al7075 alloy at 180 °C

microstructures: (1) GP zones dissolving; (2) the formation and development of small particles; and (3) primary coarsening of particles °Ccurs after coarsening of grain boundary precipitate. The GP zones are formed by congregating the dissolved copper, zinc, and magnesium in a completely coherent matrix. The semi-coherent phase has

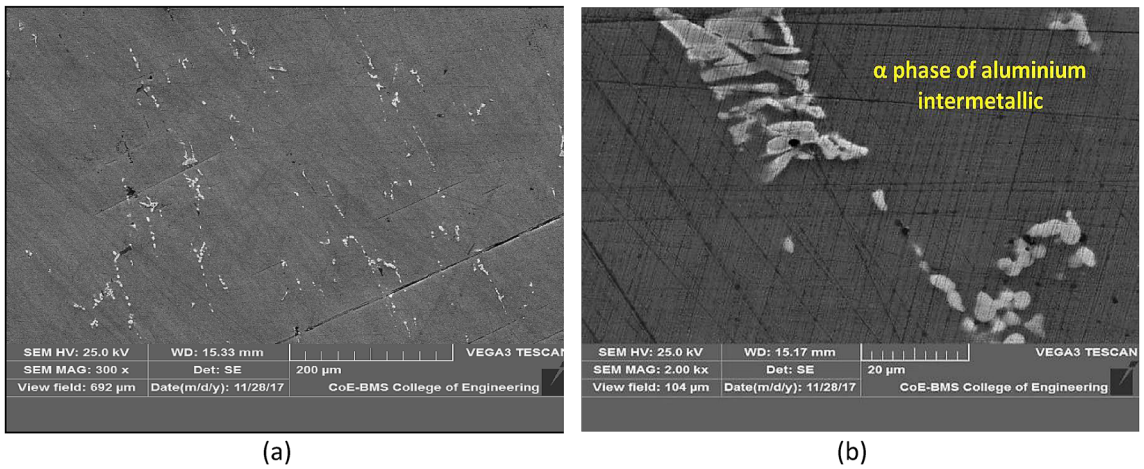

Fig. 4 **a-b** SEM of RRA-treated Al7075 alloy at 200 °C

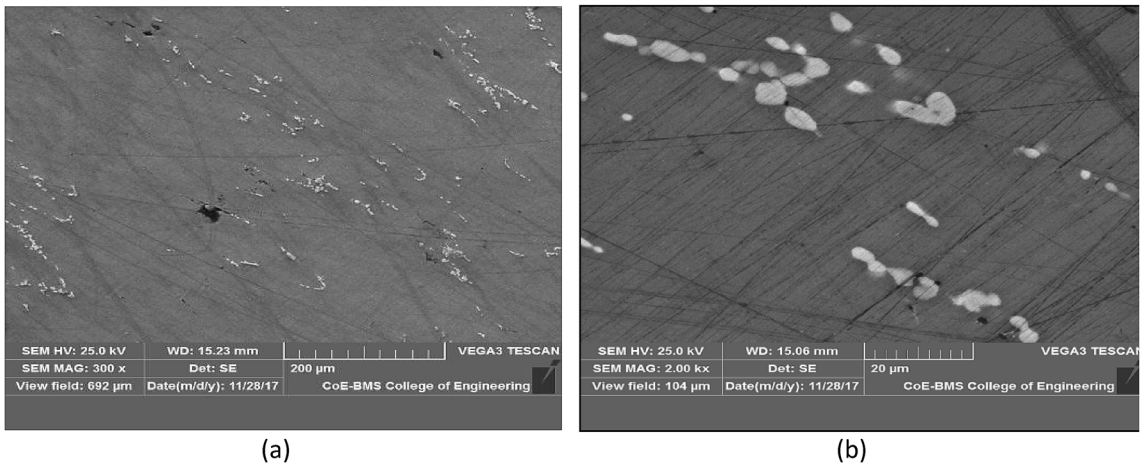

Fig. 5 **a-b** SEM of RRA-treated Al7075 alloy at 220 °C

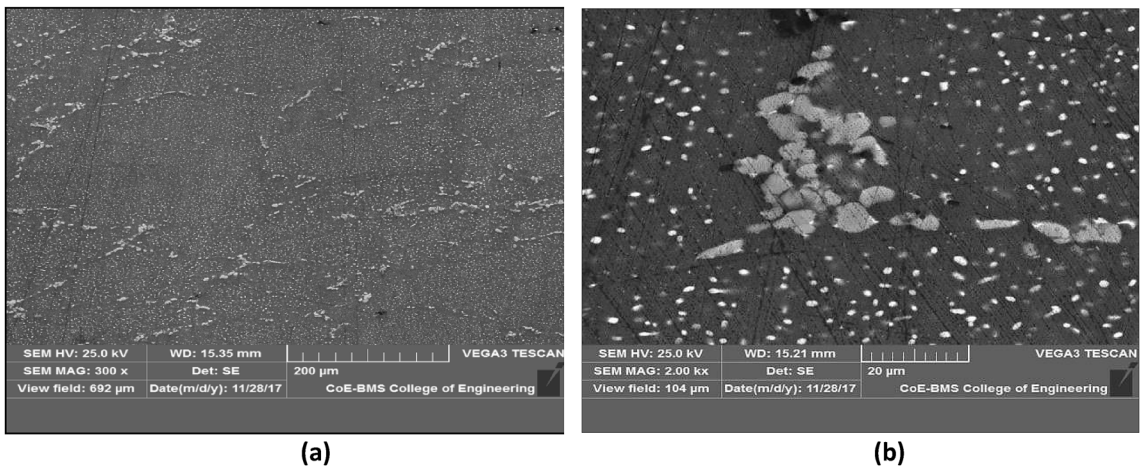

Fig. 6 **a-b** SEM of Al7075 alloy

formed in separate sheets and grains. Because it is an incoherent phase, the stable equilibrium phase settles at grain boundaries. As a result of the RRA condition of the AA7075 structure, in the T73 condition, the grains are

distributed with particles that are very thin and uniformly distributed, as well as together at the grain boundaries with ($MgZn_2$) precipitate. This type of microstructure explains why AA7075 alloy retains mechanical strength as well as corrosion resistance after RRA treatment [27].

This can be interpreted as the dispersion of Al–Zn–Mg eutectic phases caused by high temperature increasing the solubility of the matrix phase. The secondary-phase precipitates in the RRA heat-treated alloy were found to be mostly at grain boundaries. This could be due to the fact that the precipitates formed in RRA samples were denser in the structure. It was also discovered that heat treatment methods and parameters influence secondary-phase precipitate size and volume ratios.

X-Ray Diffraction Analysis

Aluminum 7075 T6 tempered and RRA heat-treated alloy was subjected to X-ray diffraction (XRD) analysis. Each specimen is subjected to retrogression and reaging (RRA) at various temperatures for 24 h. The XRD analysis of raw AA7075 specimens is also studied and compared to the XRD analysis of RRA-treated AA7075 specimens. For RRA-treated specimens, the highest peaks form at different angles of 2. These peaks contain all of the elements, including Al, Cr, Mg, Mn, and Zn. These elements are the primary components of the RRA temperature-treated specimen of AA 7075 alloy, which has increased its strength and hardness. Figures 7 and 8 show how $MgZn_2$ precipitates form during the reaging process as a result of the phase transformation from semi-coherent ($MgZn_2$) to coherent (Al, Zn, Al_2Zn_3, and Al_2Mg_3). As a result, the dendrite structure has formed, which is uniform along the grain boundaries and has equiaxed grains.

As a result, the grain boundaries are better and longer, and the precipitates within the grains are finer, resulting in an increase in the mechanical properties of RRA-treated AA 7075 alloy. It has also been discovered that coherent and semi-coherent precipitates are highly discrete in the AA7075 solid resolution, which consists primarily of zinc, magnesium, and copper. Figures 9 show that the third peak is the highest, indicating that there are more coherent precipitates present. High strength and mechanical properties are formed during RRA due to the presence of finely dispersed precipitates in the boundaries of the grains, as well as the presence of a larger capacity fraction of precipitates and less interspacing between the grains. Because of 1 precipitates, high strength and mechanical properties are formed during RRA. The presence of finely dispersed precipitates in the grain boundaries, as well as a higher capacity fraction of precipitates and less interspacing between the grains. The main precipitates are $MgZn_2$ platelets that °Ccur as grains and are semi-coherent 1 precipitates within the matrix. In RRA-treated 7075 AA, two peaks of (Al-Zn-Mg) are typically observed; the first highest graph is associated with high compactness G-P zones that are weak. The second peak represents coherent precipitates at grain boundaries. The X-ray diffraction of raw AA 7075 alloy is shown in Fig. 10. The maximum aluminum peak can be seen at 2 = 38.68. This indicates that the grain boundaries of the 7075 AA have high densities of the G-P zones. The absence of the Al_4C_3 peaks also indicates a coarser grain structure in the matrix. The XRD graphs of raw AA 7075 also show that the affinity of Zn with Mg is greater due to the formation of intermetallic

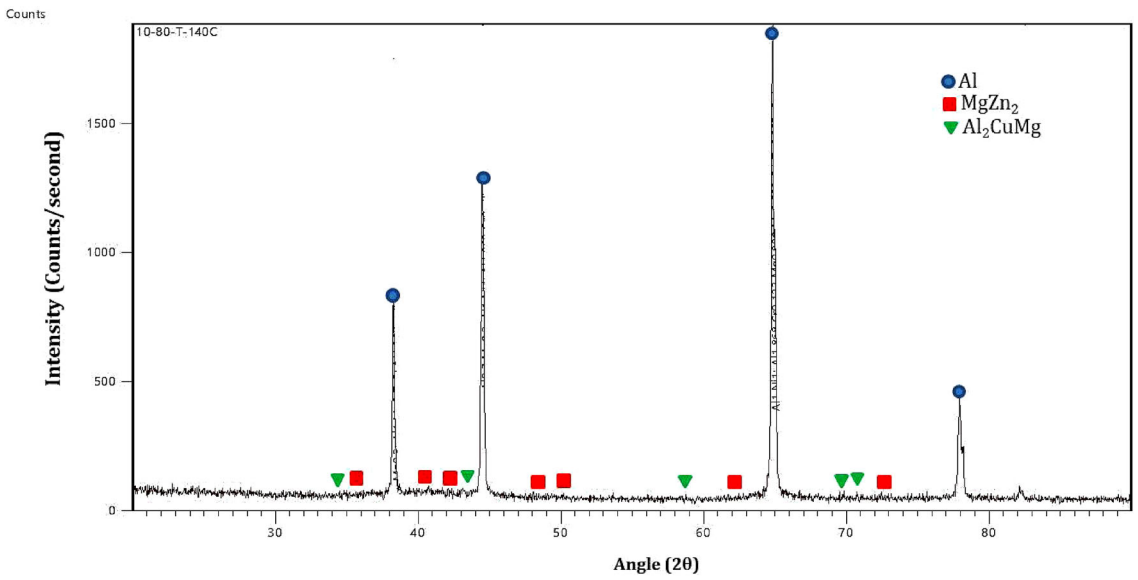

Fig. 7 X-Ray Diffractogram of 140 °C RRA-Treated AA7075 Specimen

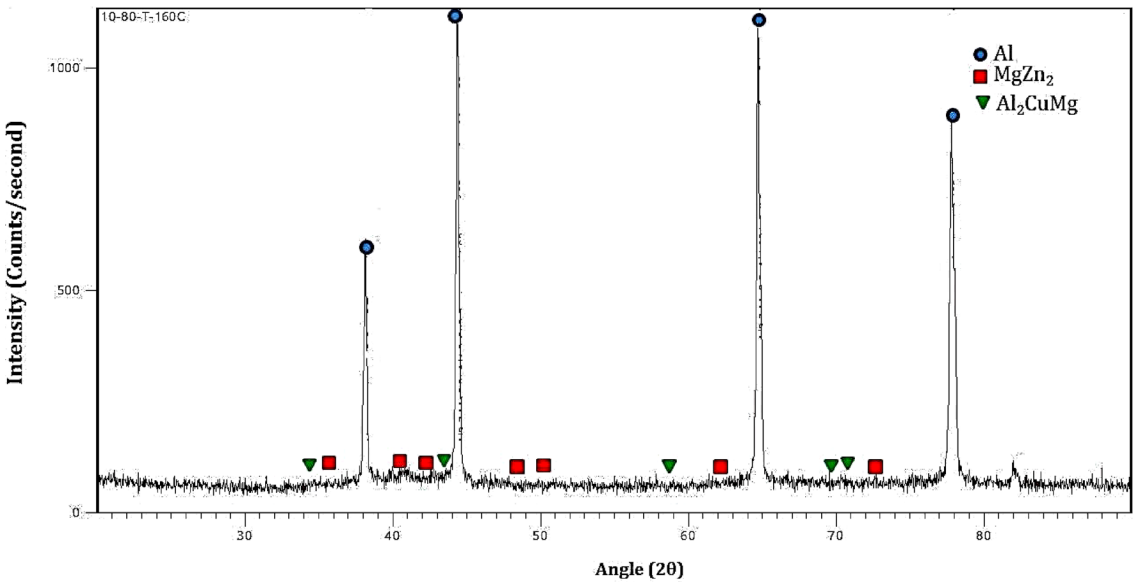

Fig. 8 X-Ray Diffractogram of 160 °C RRA-Treated AA7075 Specimen

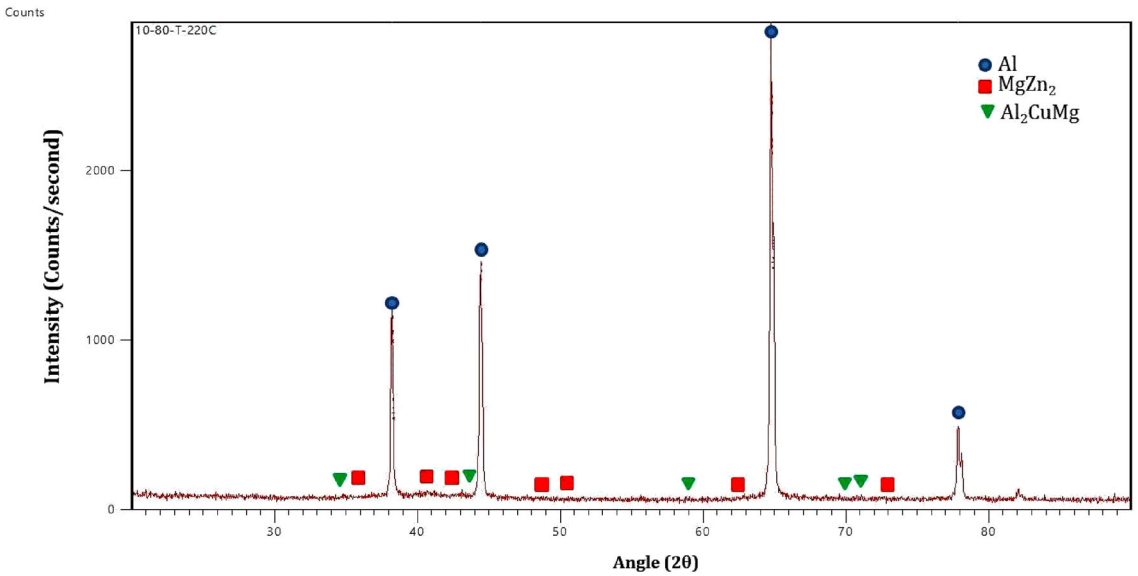

Fig. 9 X-Ray Diffractogram of 220 °C RRA-Treated AA7075 Specimen

precipitates such as Al_2CuMg, which are not distributed along the grain boundaries and are dispersed throughout the matrix, which may explain the equal peaks observed in the raw material of X-ray diffraction analysis, resulting in lower mechanical properties. Intermetallic phases such as Al_2Mg_3 and Al_2CuMg are shaped around dendrites at grain boundaries, making the grains sharper and brittle. The XRD results show that matrix phase, Al_2Cu, and $MgZn_2$ phases are formed in the alloys structure. Previous research has also discovered that the $MgZn_2$ phase, expressed as stable and incoherent, exists in the structure of AA7075 alloys.

Hardness

As shown in Fig. 11, hardness decreases steadily as the duration and temperature of the retrogression increase. The hardness decline slope decreases with increasing duration. The first reduction in hardness is associated with the start of the dissolution of semi-coherent phase as well as fully coherent (GP zones). A further increase in hardness may be observed at the beginning of retrogression (until the first ten minutes). This is due to the formation of the newly nucleated phase across dissolved GP regions. This phase's increase in volume ratio, which is significantly greater than

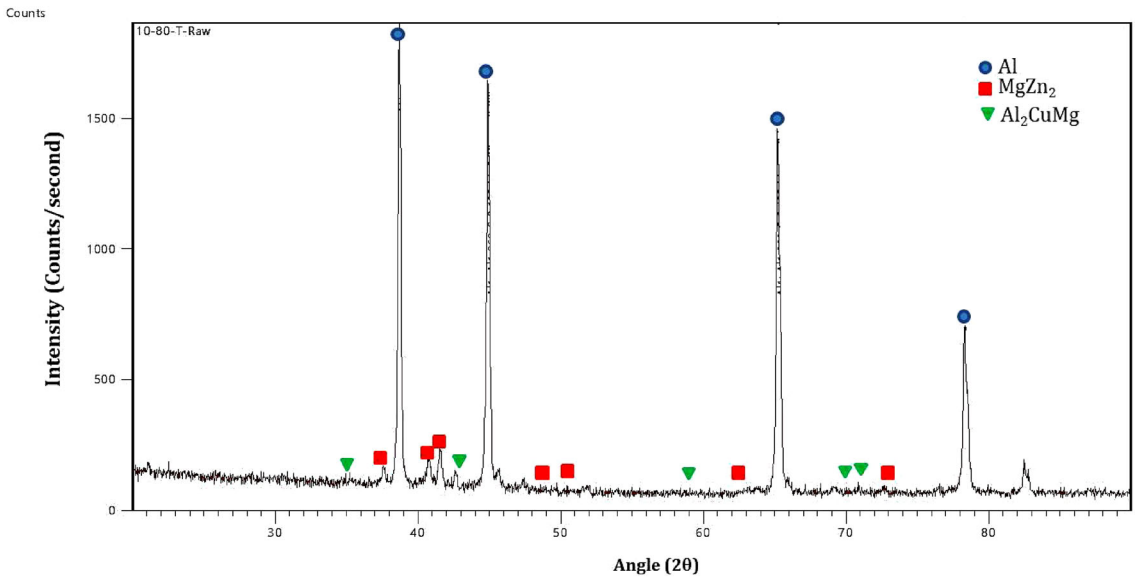

Fig. 10 X-Ray Diffractogram of AA7075 Raw Specimen

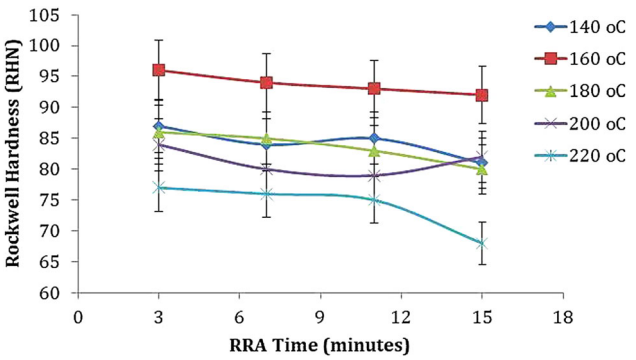

Fig. 11 Effect of RRA temperature and time on hardness of aluminum 7075 alloy

that of the T651 condition, provides superior hardness to the T651 condition. As the duration of the retrogression process increases, the phase transforms into a phase of stable equilibrium (phase). As a result of this incoherent phase, the hardness decreases once more. This issue of hardness is sometimes interpreted as being related to aging [28–31].

The formation of precipitate in the microstructure, as well as its dispersion, is related to an increase in toughness as well as an increase in duration time. In the dissolved GP zones, the distribution of volume per unit of newly generated phase is thinner and denser with respect to time and heat temperature. The hardness achieved in this situation is greater than the hardness achieved in the T651 condition. With a result like this, the impact toughness is also increased. Nonetheless, as time passes, this phase causes semi-coherent phase transitions to the phase of stable equilibrium (phase), and this phase causes a hardness decrease due to its incoherency. The hardness decreases as the retrogression time increases despite the incoherent phase formations. The reasons for this are as follows. The increase in impact toughness as well as the increase in retrogression time occurs as a result of the RRA condition ending, at grain boundaries coarsens precipitates a continuous as well as correspondingly smaller stable equilibrium and it transforms into discontinuous. In this way, the coarse forming as well as the discontinuous phase transforms the previously blocked grain boundary line. The energy values in the area have changed as a result of the removal of the continuous net structure. Furthermore, the notch effect is reduced by the hard and brittle continuous net phase at the grain boundary. The precipitate increases hardness in this area of high energy, which is found at grain boundaries in continuous net form in the condition of T651, but it causes a high notch effect because the precipitate is continuous. The continuous net phase at the grain boundary is shattered as the heat temperature and time increase after T651. The continuous net phase breaking causes the precipitate to coarsen and become spherical as time and heat temperature increase. As a result, free energy is increased during continuous net phase removal from high energy grain boundaries, and the notch effect is reduced in the structure by the spherical precipitate. In terms of the aforementioned factors, hardness decreases with increasing time or temperature while strength increases [32–35].

The hardness of the RRA heat-treated and annealed AA7075 alloys is shown in Fig. 11. The hardness value of the heat-treated AA7075 alloy of RRA was nearly twice that of the annealed hardness samples. The aging heat treatment, which is well known for this function, significantly increases the hardness of the AA7075 alloy. The

hardness of the AA7075 alloy is known to increase with the formation of second-phase precipitates in the matrix caused by aging heat treatments. The mechanism of strengthening can be described broadly as an impediment to the movement of dislocations in the matrix by secondary-phase particles. According to a previous study, the precipitates in T6 heat-treated alloys show a continuous distribution as well as an intense distribution at grain boundaries [36–38]. The size of the secondary-phase precipitates enlarges with reaging, resulting in a slight decrease in hardness. The hardness of the tensile tested samples decreased as the temperature rose. The annealed alloy's hardness decreased as the test temperature increased. Similarly, the hardness of RRA heat-treated samples was reduced. This is due to grain coarsening caused by material overaging as a result of elevated temperatures. The hardness results show that the RRA heat-treated samples outperformed the annealed samples in terms of hardness.

Tensile Strength

Tensile tests were performed on various test specimens that had been aged at 120 °C for 24 h and then retrograted at various temperatures of 140, 160, 180, 200 and 220 °C for different time intervals of 3 min, 7 min, 11 min, and 15 min. These specimens are reaged at 120 °C for another 24 h. Figure 12 depicts the values of ultimate tensile strength (UTS) for various retrogression times (mins) and RRA temperatures. The graph shows that as retrogression and reaging (RRA) time increases, Ultimate tensile stress (UTS) decreases for all samples at various RRA temperatures of 140, 160, 180, 200 and 220 °C. When compared to other RRA temperature specimens, the UTS for RRA temperature of 160 °C is high. The UTS value of RRA-treated specimens appears to be higher than the UTS value of as-cast 7075 alloy without heat treatment. This is due to an increase in strength caused by finely dispersed semi-coherent phase and equilibrium phase precipitates within

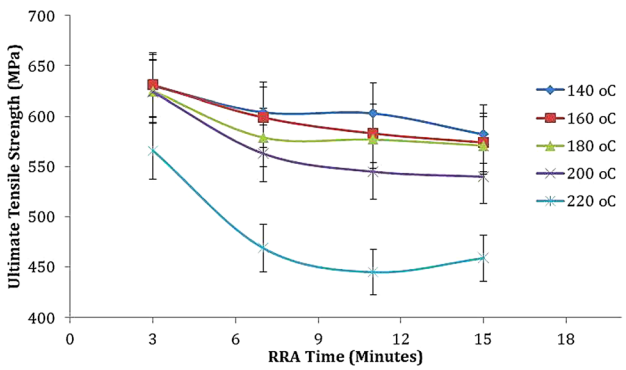

Fig. 12 Effect of RRA temperature and time on ultimate tensile strength

and along AA7075 alloy grain boundaries during heat treatment. The RRA treatment causes initial coarsening of the grain boundaries, which increases volume per unit grain boundary area. The partial dissolution reduces the yield strength, which is then gained by reaging. Zinc content has also contributed to an increase in tensile strength. Figure 12 shows that the UTS of the RRA-treated specimens at 180, 200 and 220 °C has decreased. Because of the presence of Guinier–Preston (GP) zones, this is the case.

The tensile strength of the annealed samples at room temperature was 183.536 and 274.245 MPa. The RRA heat-treated AA7075 alloy samples had a tensile strength of 548.564 MPa. These results show that RRA heat treatment resulted in a significant increase in strength. RRA heat treatment reduced the elongation of the AA7075 alloy from 19.219 to 12.771 after it was annealed at room temperature. This increasing strength could be due to the influence of high temperature on stable incoherent secondary phases becoming coherent with the matrix. As the temperature rises, both the annealed and RRA heat-treated samples lose strength while increasing ductility. There was an increase in elongation of approximately 124% in the annealed samples and 19% in the RRA heat-treated samples when compared to the characteristics of the samples tensile tested at room temperature and higher temperature. The ductility increase in the annealed samples was much greater than in the RRA-treated samples. The mechanical properties of RRA-treated samples at elevated temperatures were found to be nearly identical to the mechanical properties of annealed samples at room temperature. Metals' mechanical properties are known to degrade as temperature rises. The movement of the dislocations increases as the deformation temperature rises, resulting in a decrease in flow stress. For AA7075 alloy, the recrystallization temperature is estimated to be around 300 °C at approximately 0.3–0.4Tm. Increasing the temperature of deformation promotes grain growth and results in larger recrystallized grains. Recrystallization is regarded as the primary softening mechanism at high deformation temperatures. Mechanical properties of RRA heat-treated AA7075 alloy samples showed a negligible decrease in strength. This is due to the coarser and greater amount of secondary-phase precipitates formed in the RRA heat-treated AA7075 alloy samples as a result of the longer heat treatment exposure via retrogression and reaging. A comparable case is the increase in the size of secondary phases in the structure over long aging times [39–44].

Percentage of Elongation

Tensile tests were performed to determine the percentage of elongation for various test specimens that had been aged at 120° C for 24 h and then retrograted at different

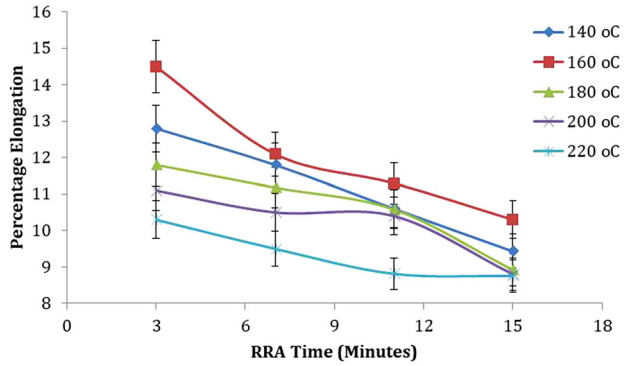

Fig. 13 Effect of RRA temperature and time on Percentage elongation

temperatures of 140, 160, 180, 200 and 220° C for 3 min, 7 min, 11 min, and 15 min of varying time intervals. These specimens are reaged at 120° C for another 24 h. Figure 13 depicts the elongation percentage values for various retrogression times in minutes (mins) and RRA temperatures.

Figure 13 depicts a graph plotted for percentage of elongation vs. retrogression time (mins). For temperatures of 140, 160, 180, 200 and 220° C, the percentage of elongation for retrogression time of 3 min is higher than for retrogression time of 7 min, 11 min, and 15 min. The ductility of the specimen increased after 3 min of retrogression at temperatures of 140, 160, 180, 200 and 220° C. The highest percentage of elongation can be seen for the 1600 C RRA specimens, while the lowest percentage of elongation can be seen for the RRA-treated specimen at 220° C. The same specimen also has the lowest ultimate tensile strength (UTS) values, whereas the specimen aged at RRA temperature of 160° C has a higher percentage of elongation and tensile strength than the other specimens. This indicates that the ductility of these specimens has increased when compared to the 180, 200, and 220° C specimens, resulting in an increase in UTS.

Conclusions

The microstructure of the as-cast specimen contains the -Al + Eutectic phase (dark) in the -Al matrix (light), as well as the eutectic phase at grain boundaries. The precipitates in the aluminum matrix of uniformly dispersed second-phase components comprise the solutionized as well as the age-hardened microstructure. During the treatment of reaging and retrogression, the matrix is re-precipitated, and the coarsened grain boundary precipitates. Because less stable precipitates were dissolved during retrogression treatment, they can develop as the grain boundary precipitates become more stable. Reaging improves one-phase re-precipitation as a result.

As the retrogression period increases, the hardness and ultimate tensile strength decrease. Hardness and tensile strength increase first and subsequently decrease as temperature rises. For the entire retrogression duration, a higher percentage of elongation was recorded for 160 °C. However, as time passes, the percentage elongation for all temperatures decreases.

Funding No funding was received for this work.

Declarations

Conflict of interest The authors declare that there is no conflict of interest.

References

1. M. Zhou, Y.C. Lin, J. Deng, Y.Q. Jiang, Hot tensile deformation behaviors and constitutive model of an Al-Zn-Mg-Cu alloy. Mater. Des. **59**, 141–150 (2014)
2. W.G. Moffatt, G.W. Pearsall, J. Wulff, *The Structure and Properties of Materials* (Structure, Wiley, New York, 1967)
3. W.S. Lee, W.C. Sue, C.F. Lin, C.J. Wu, The strain rate and temperature dependence of the dynamic impact properties of 7075 aluminum alloy. J. Mater. Process. Technol. **100**(1–3), 116–122 (2000)
4. T. Kobayashi, Strength and fracture of aluminum alloys. Mater. Sci. Eng. A **286**(2), 333–341 (2000)
5. P.K. Rout, M.M. Ghosh, K.S. Ghosh, Microstructural, mechanical and electrochemical behaviour of a 7017 Al-Zn-Mg alloy of different tempers. Mater. Charact. **104**, 49–60 (2015)
6. E. Maire, S. Zhou, J. Adrien, M. Dimichiel, Damage quantification in aluminium alloys using in situ tensile tests in x-ray tomography. Eng. Fract. Mech. **78**(15), 2679–2690 (2011)
7. O. Gokhen, A. Karaaslan, Properties of AA 7075 aluminium alloy in aging and retrogression and reaging process. Transactions Nonferrous Metal Soc. China **27**, 2357–2362 (2017)
8. M. Esmailian, M. Shakouri, A. Mottahedi, S.G. Shabestari, Effect of T6 and re-aging heat treatment on mechanical properties of 7055 aluminum alloy. Int. J. Mater. Metall. Eng. **9**(11), 1303–1306 (2015)
9. Y. Reda, R. Abdel-Karim, Improvements in mechanical and stress corrosion cracking properties in aluminium alloy 7075 via retrogression and reaging. Mater. Sci. Eng. **A85**, 468–475 (2008)
10. X.L. Zou, H. Yan, X.H. Chen, Evolution of second phases and mechanical properties of 7075 Al alloy processed by solution heat treatment. Trans. Nonferrous Met. Soc. China (Engl Ed) **27**(10), 2146–2155 (2017)
11. H.B. Zhang, B. Wang, Y.T. Zhang, Y. Li, J.L. He, Y.F. Zhang, Influence of aging treatment on the microstructure and mechanical properties of CNTs/7075 Al composites. J. Alloys Compd. **814**, 152357 (2020)
12. S.H. Jung, J. Lee, M. Kawasaki, Effects of pre-Strain on the aging behavior of Al 7075 alloy for hot-stamping capability. Metals (Basel) **8**(2), 137 (2018)
13. C.P. Ferrer, M.G. Koul, B.J. Connolly, A.L. Moran, Improvements in strength and stress corrosion cracking properties in aluminum alloy 7075 via low-temperature retrogression and reaging heat treatments. Corrosion **59**(6), 520–528 (2003)
14. M. Yildirim, D. Özyürek, M. Gürü, The effects of precipitate size on the hardness and wear behaviors of aged 7075 aluminum

alloys produced by powder metallurgy route. Arab. J. Sci. Eng. **41**(11), 4273–4281 (2016)
15. N.C. Danh, K. Rajan, W. Wallace, A TEM study of microstructural changes during retrogression and reaging in 7075 aluminum [J]. Metall. Trans. A **14**, 1843–1850 (1983)
16. J.K. Park, A.J. Ardell, Effect of retrogression and reaging treatments on the microstructure of Al-7075-T651. Metall. Trans. A **15–18**, 1531–1543 (1984)
17. W. Lacom, Calorimetric investigations strengthened 7075 in a dispersion alloy. Thermochim. Acta **271**, 93–100 (1996)
18 P.N. Adler, R. Delasi, Calorimetric studies of 7000 series aluminum alloys: II comparison of 7075, 7050, and RX720 alloys. Metall. Transactions A **8**, 1185–1190 (1977)
19. F. Fandreatta, H. Terryn, J.H.W. de Wit, Effect of solution heat treatment on galvanic coupling between intermetallics and matrix in AA7075-T6 [J]. Corros. Sci. **45**, 1733–1740 (2003)
20. N.C. Danh, K. Rajan, W. Wallace, A TEM study of microstructural changes during retrogression and reaging in 7075 aluminum. Metall. Trans. A **14**, 1843–1850 (1983)
21. F. Fandreatta, H. Terryn, J.H.W. de Wit, Effect of solution heat treatment on galvanic coupling between intermetallics and matrix in AA7075-T6. Corros. Sci. **45**, 1733–1740 (2003)
22. F. Viana, A.M.P. Pinto, H.M.C. Santos, A.B. Lopes, Retrogression and re-ageing of 7075 aluminium alloy: microstructural characterization. J. Mater. Process. Technol. **92–93**, 54–59 (1999)
23. N.C. Danh, K. Rajan, W. Wallace, A TEM study of microstructural changes during retrogression and reaging in 7075 aluminum. Metall Trans A **14**(9), 1843–1850 (1983)
24. K. Rajan, W. Wallace, J.C. Beddoes, Microstructural study of a high strength stress-corrosion resistant 7075 aluminum alloy. J Mat Sci **17**, 2817–2824 (1982)
25. B.M. Cina, B. Ranish, *A new technique for reducing susceptibility to stress corrosion of high strength aluminum alloys* (American Society for Metals, Pittsburgh, Aluminum Industrial Products, 1974)
26. H.R. Zaid, A.M. Hatab, A.M.A. Ibrahim, Properties enhancement of Al−Zn−Mg alloy by retrogression and re-aging heat treatment. J. Min. Metall. Sect. B Metall. **47**(1), 31–35 (2011)
27. . B.M. Cina, (1974) Reducing the susceptibility of alloys, particularly aluminum alloys to stress corrosion cracking. U.S. Patent 3,856,584
28. J.P. Immarigeon, R.T. Holt, A.K. Koul, L. Zhao, W. Wallace, J.C. Beddoes, Lightweight materials for aircraft applications. Mater Char **35**(1), 41–67 (1995)
29. J.K. Park, A.J. Ardell, Microstructure of the commercial 7075 Al alloy in the T651 and T7 tempers. Metall Trans A **14A**, 1957–1966 (1983)
30 Y.C. Lin, J.L. Zhang, G. Liu, Y. Liang, Effects of pre-treatments on aging precipitates and corrosion resistance of a creep-aged Al−Zn−Mg−Cu alloy. Mater. Design **83**, 866–875 (2015)
31. M.J. Starink, S.C. Wang, A model for the yield strength of overaged Al−Zn−Mg−Cu alloys. Acta Mater. **51**, 5131–5150 (2003)
32. C.W. Bartges, Changes in solid solution composition as a function of artificial ageing time for aluminium alloy 7075. J. Mater. Sci. Lett. **13**, 776–778 (1994)
33. P.E.N.G. Guo-sheng, C.H.E.N. Kang-hua, C.H.E.N. Song-yi, F.A.N.G. Hua-chan, Influence of dual retrogression and re-aging condition on microstructure strength and exfoliation corrosion behavior of AlZnMgCu alloy. Transactions Nonferrous Metals Soc. China **22**, 803–809 (2012)
34. G. Sha, A. Cerezo, Early-stage precipitation in Al−Zn−Mg−Cu alloy (7050) [J]. Acta Mater. **52**, 4503–4516 (2004)
35. X. Xu, Y. Zhao, B. Ma, M. Zhang, Electropulsing induced evolution of grain-boundary precipitates without loss of strength in the 7075 Al alloy. Mater. Charact. **105**, 90–94 (2015)
36. A. Deschamps, Y. Brechet, Influence of quench and heating rates on the ageing response of an Al−Zn−Mg−(Zr) alloy. Mater. Sci. Eng., A **251**, 200–207 (1998)
37. K.K. Ma, H.M. Wen, H.U. Tao, T.D. Topping, D. Isheim, D.N. Seidman, E.J. Lavernia, J.M. Schoenung, Mechanical behavior and strengthening mechanisms in ultrafine grain precipitation-strengthened aluminum alloy [J]. Acta Mater. **62**, 141–155 (2014)
38. M.J. Starink, X.M. Li, A model for the electrical conductivity of peak-aged and overaged Al−Zn−Mg−Cu alloys. Metall. Mater. Trans. A. **34**, 899–911 (2003)
39. H. Fooladfar, B. Hashemi, M. Younesi, The effect of the surface treating and high-temperature aging on the strength and SCC susceptibility of 7075 aluminum alloy. J. Mater. Eng. Perform. **19**(6), 852–859 (2010)
40. T. Marlaud, B. Malki, C. Henon, A. Deschamps, B. Baroux, Relationship between alloy composition, microstructure and exfoliation corrosion in Al−Zn−Mg−Cu alloys. Corros. Sci. **53**, 3139–3149 (2011)
41. Y. Reda, R. Abdel-Karim, I. Elmahallawi, Improvements in mechanical and stress corrosion cracking properties in Al-alloy 7075 via retrogression and re-aging. Mater. Sci. Eng. A **485**, 468–475 (2008)
42. A.F. Oliveira Jr., M.C. de Barros, K.R. Cardoso, D.N. Travessa, The effect of RRA on the strength and SCC resistance on aluminium alloys. Mater. Sci. Eng. A **379**, 321–326 (2004)
43. M. Chemingui, M. Khitouni, K. Jozwiak, G. Mesmacgue, A. Kolsi, Characterization of the mechanical properties changes in an Al–Zn–Mg alloy after a two-step ageing treatment at 70 °C and 135 °C. Mater. Des. **31**, 3134–3139 (2010)
44. T. Marlaud, A. Deschamps, F. Bley, W. Lefebvre, B. Baroux, Evolution of precipitate microstructures during the retrogression and re-ageing heat treatment of an Al−Zn−Mg−Cu alloy. Acta Mater. **58**, 4814–4826 (2010)